

An Anomalous Phase in the Relaxor Ferroelectric $\text{Pb}(\text{Zn}_{1/3}\text{Nb}_{2/3})\text{O}_3$

Guangyong Xu,¹ Z. Zhong,¹ Y. Bing,² Z.-G. Ye,² C. Stock,³ and G. Shirane¹

¹Brookhaven National Laboratory, Upton, New York 11973

²Department of Chemistry, Simon Fraser University, Burnaby, British Columbia, Canada, V5A 1S6

³Department of Physics, University of Toronto, Toronto, Ontario, Canada M5S 1A7

(Dated: November 15, 2018)

X-ray diffraction studies on a $\text{Pb}(\text{Zn}_{1/3}\text{Nb}_{2/3})\text{O}_3$ (PZN) single crystal sample show the presence of two different structures. An outer-layer exists in the outer most ~ 10 to $50 \mu\text{m}$ of the crystal, and undergoes a structural phase transition at the Curie temperature $T_C \approx 410$ K. The inside phase is however, very different. The lattice inside the crystal maintains a cubic unit cell, while ferroelectric polarization develops below T_C . The lattice parameter of the cubic unit cell remains virtually a constant, i.e., much less variations compared to that of a typical relaxor ferroelectric, in a wide temperature range of 15 K to 750 K. On the other hand, broadening of Bragg peaks and change of Bragg profile line-shapes in both longitudinal and transverse directions at T_C clearly indicate a structural phase transition occurring.

PACS numbers: 77.80.-e, 77.84.Dy, 61.10.-i, 61.10.Nz

I. INTRODUCTION

$\text{Pb}(\text{Zn}_{1/3}\text{Nb}_{2/3})\text{O}_3$ (PZN) is a typical relaxor with a broad and strongly frequency-dependent dielectric constant ϵ . When doped with PbTiO_3 (PT), forming solid solutions of PZN- x PT, the piezoelectric properties are greatly enhanced^{1,2,3}. The great potential for industrial applications inspired a series of studies on the PT doped systems. One of the most important among those was the discovery of a monoclinic phase which is directly related to the high piezoelectric response^{4,5,6,7}. Pure PZN itself was believed to undergo a cubic-to-rhombohedral phase transition upon cooling with zero-field at the Curie temperature $T_C \approx 410$ K. Nevertheless, very few direct structural studies on PZN have been reported for a long time. Only recently, Lebon *et al.* performed the first explicit zero-field x-ray diffraction measurements on pure PZN single crystals⁸. They observed the transformation into the rhombohedral phase at T_C , as previously believed. As shown in Fig. 1, the phase transition occurs at about the same temperature where the dielectric constant ϵ peaks, and the rhombohedral distortion develops with cooling.

However, more recent high energy (67 keV) x-ray diffraction measurements by Xu *et al.* revealed the existence of a different phase⁹. 67 keV x-ray beams can penetrate deeply into the sample and therefore probe the inside of the crystal. It was found that the structure inside of the pure PZN single crystal has an undistorted lattice (unit cell shape) instead. The true symmetry (atomic shifts) of the structure was not yet determined, and this unidentified phase was named “phase X”. On the other hand, an outer-layer of about 10 to 50 μm was found to exist and have a different structure than the inside of the crystal. At room temperature ($T < T_C$), the outer-layer has a rhombohedrally distorted structure, consistent with results by Lebon *et al.* This suggests that previous x-ray diffraction measurements with x-ray energies around 10 keV only measure the outer-layer structure, as do pow-

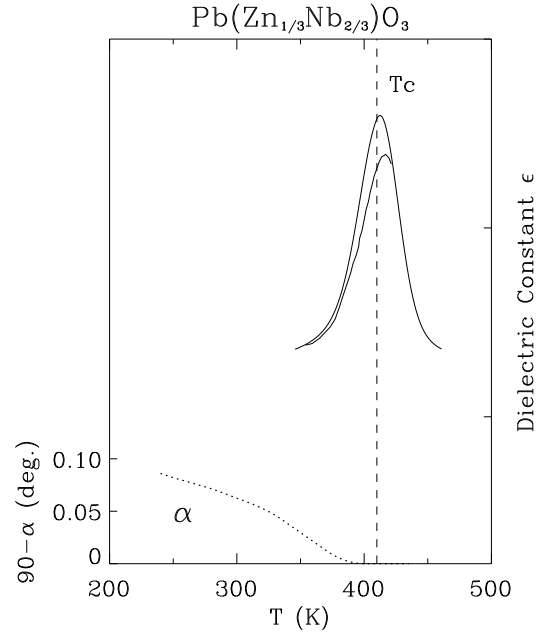


FIG. 1: Schematic of the frequency dependent dielectric constant ϵ , and the rhombohedral distortion angle $90^\circ - \alpha$ (by Lebon *et al.*⁸) for pure PZN, plotted vs. temperature T . The vertical dashed line indicate the Curie temperature T_C .

der diffraction measurements, since the average grain size of powder samples is $\sim 50 \mu\text{m}$. Most recent x-ray studies have found similar inside/outer-layer type structures in PZN-4.5%PT and PZN-8%PT¹⁰.

Phase X is extremely unusual in many aspects. Neutron scattering measurements by Stock *et al.*¹¹ on a pure PZN single crystal show that the (300) Bragg intensity increases significantly at T_C upon cooling. This can be explained by a symmetry lowering and therefore release of extinction effect in the system. In addition, both longitudinal and transverse width of the Bragg peak measured

show broadening effects at the phase transition temperature T_C . All of these indicate that although there is no rhombohedral lattice distortion in phase X, a structural phase transition does occur at T_C .

In this paper, we present detailed high energy (67 keV) x-ray diffraction measurements on single crystal PZN. Our results show that the phase (X) inside of the crystal behaves very differently than a normal ferroelectric phase. In spite of the absence of rhombohedral distortions, strain and effective sample mosaic both develop with cooling below T_C . However, the lattice parameter a of phase X appears to be virtually a constant over a large temperature range of 15 K to 750 K, quite contrary to the thermal expansion of typical ferroelectric oxide systems.

II. EXPERIMENT

The PZN single crystal used in our measurements is the same unpoled crystal used in Ref. 9, grown at the Simon Fraiser University. The dimensions are $3 \times 3 \times 1$ mm³. High energy x-ray diffraction measurements were carried out at X17B1 beamline of the National Synchrotron Light Source (NSLS). The x-ray energy at X17B1 beamline is 67 keV, with an attenuation length of ~ 400 μ m in PZN. The measurements were performed in the transmission mode to ensure that the inside of the crystal is being probed. Measurements on the “outer-layer” structure were done with x-ray energy of 10.2 keV at X22A beamline of the NSLS. In this case the x-ray attenuation length is only ~ 10 μ m and the diffraction measurements were done in the reflection mode instead. Careful wavelength calibrations have been done on both beam lines with perfect Si and Ge crystals. Our measurements were carried out in the temperature range of 15 K to 750 K. The sample holder was specially redesigned to minimize external strain on the sample.

III. RESULTS

In a rhombohedral phase, the lattice is stretched along the body diagonal direction. Therefore, the $\{111\}$ Bragg peaks should be most sensitive to the rhombohedral distortion, and split due to the two $\{111\}$ lengths in different domains of the crystal. In Fig. 1, longitudinal scans ($\theta - 2\theta$ scans) through the (111) Bragg peak are shown. The units are multiples of the reciprocal lattice unit $a^* = 2\pi/4.067 \text{ \AA} = 1.545 \text{ \AA}^{-1}$. When probed with 67 keV x-rays, the inside of the crystal shows no sign of rhombohedral distortion. The (111) Bragg peak remains single and sharp both above and below T_C . In contrast to neutron scattering measurements on the (110) and (200) Bragg peaks¹¹, no longitudinal broadening was observed by 67 keV x-ray measurements on the (111) Bragg peak. The three $\{200\}$ Bragg peaks were also re-visited at room temperature ($T < T_C$) to examine the previously observed slight tetragonal distortion⁹. The difference be-

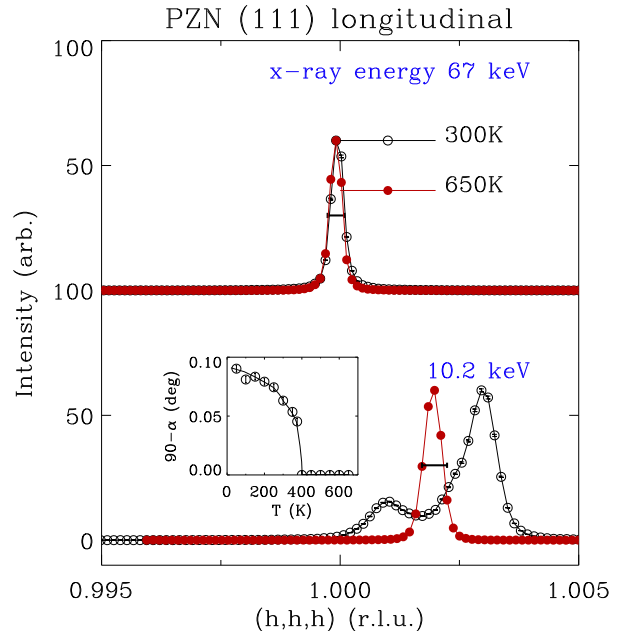


FIG. 2: Longitudinal scans through the (111) Bragg peak, measured at temperatures above and below T_C . The top panel are diffraction results using 67 keV x-rays, and the bottom panel with 10.2 keV x-rays. The inset shows the rhombohedral distortion angle derived from the 10.2 keV x-ray results. The horizontal bars indicate the instrument resolutions.

tween the lengths of three axis a , b , and c is less than 0.02%. This confirms that phase X has an average cubic unit cell shape ($a = b = c$), and previously observed tetragonal distortion (c slightly larger than a) was likely due to external strain created by the sample mount.

When looking at the outer-layer with 10.2 keV x-ray beams, a splitting of the (111) peak occurs below T_C . Assuming a rhombohedral structure, the lattice parameter and rhombohedral distortion angle can be calculated based on the positions of the two split peaks. As shown in the inset of Fig. 2, the rhombohedral distortion in the outer-layer starts to appear at T_C , and develops upon cooling, consistent with previous reports from Lebon *et al.*⁸.

Fig. 3 shows lattice parameter $a = Volume^{1/3}$, derived from our measurements, assuming a cubic lattice for the inside structure, and rhombohedral lattice for the outer-layer (below T_C). There is a $\leq 0.05\%$ systematic error between measurements on the two beamlines due to wave-length and $2\theta_0$ calibrations. For normal ferroelectric oxides, the lattice parameter decreases almost linearly on cooling down to T_C , then increases in the ferroelectric region, and decreases again, with a smaller slope. The typical thermal expansion coefficient α is in the order of 10^{-6} in the high temperature range. This is the behavior observed in the outer-layer structure, by our 10.2 keV x-ray measurements, as well as Cu K $_{\beta}$ x-

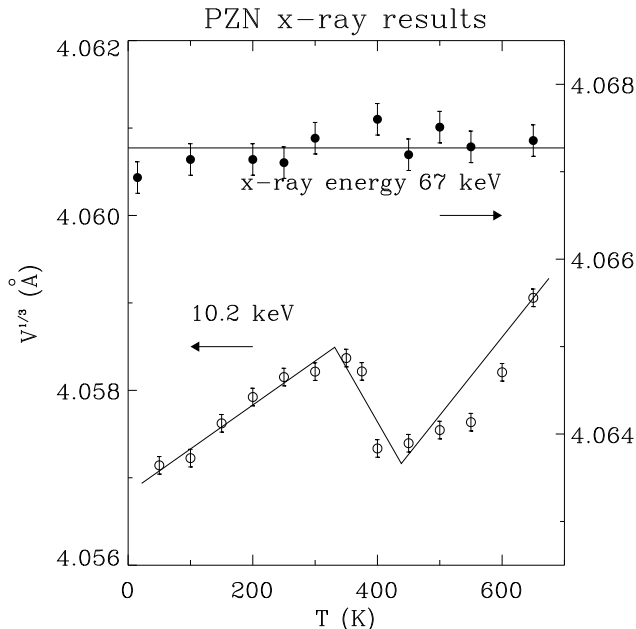


FIG. 3: Lattice parameter $a = Volume^{1/3}$, measured by 67 keV x-rays (inside) and 10.2 keV x-rays (outer-layer).

ray measurements by Lebon *et al.* Recent measurements by Bing *et al.*¹² have also provided more detailed information on the structural properties of this outer-layer. However, the temperature dependence of the lattice parameter of the inside structure, phase X, is quite different and very intriguing. Compared with that of the outer-layer, the lattice parameter of the inside appears to be $\sim 0.2\%$ larger. It also shows much less temperature variation than that of the outer-layer. The accurate thermal expansion coefficient for the inside lattice cannot be determined from our data but we can still put an upper limit that $|\alpha_{inside}| < 10^{-7}$ even in the high temperature range.

The crystal effective mosaic around the (111) Bragg peak was also measured by transverse scans (θ scans). Typical transverse scans around the (111) peak are shown in Fig. 4. With 67 keV x-rays probing inside of the crystal, the (111) transverse Bragg profile clearly changes in shape. Although the Full Width at Half Maximum (FWHM) does not appear to change much upon cooling, the profile apparently gains more spectral weight in the tails for T below T_C . In fact, instead of the Gaussian type line shape for the high temperature cubic phase, transverse (111) scans at T below T_C in phase X yield results that can be better described with a Lorentzian type line shape. On the other hand, 10.2 keV x-ray results show very little change in the (111) transverse profiles from the outer-layer.

Here we note that the FWHM of the transverse scan, or, “mosaic” (η), of the outer-layer is much greater than that of the inside. At $T = 300$ K, $\eta_{inside} \sim 0.0048^\circ$, and $\eta_{outerlayer} \sim 0.0191^\circ$. With the instrument resolution

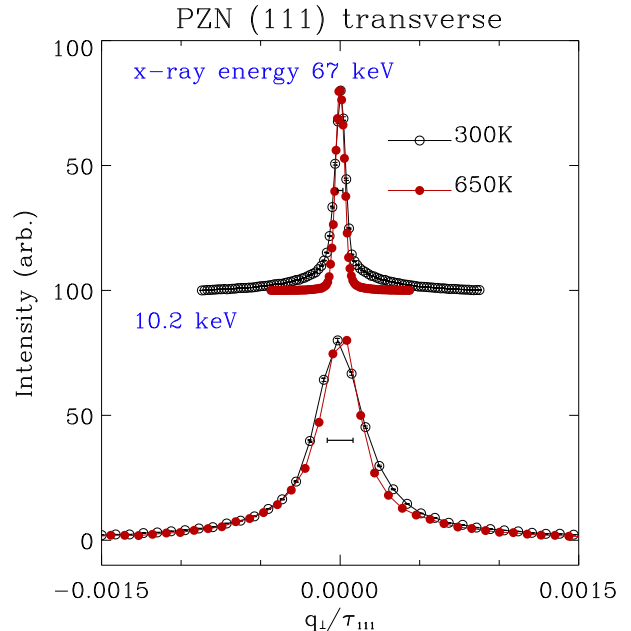


FIG. 4: Transverse scans through the (111) Bragg peak, measured at temperatures above and below T_C . The top panel are diffraction results using 67 keV x-rays, and the bottom panel with 10.2 keV x-rays. The horizontal bars indicate the instrument resolutions.

taken out ($\delta_\theta \sim 0.002^\circ$ for 67 keV x-rays, and $\delta_\theta \sim 0.0093$ for 10.2 keV x-rays), the effective mosaic of the outer-layer is about four times that of the inside. With 67 keV x-rays, although both the inside and the outer-layer are in the beam and contribute to the total diffraction intensity, the much smaller volume (about 1% to 10%) of the outer-layer, and more spread out of its diffraction intensity in θ due to the coarser mosaic, make it extremely difficult for the outer-layer to be detected. The 67 keV x-ray diffraction results are therefore dominated by those from the inside structure.

We have also performed similar longitudinal and transverse measurements with 67 keV x-rays on the (002) Bragg peak of the inside structure. In Fig. 5, longitudinal and transverse scans through the (002) Bragg peak are shown, at temperatures above and below T_C . The temperature dependence of the lattice parameter agree perfectly with that obtained by the (111) scans. Nevertheless, the change of Bragg profile width and shape at T_C becomes more significant around the (002) peak. Upon cooling, in addition to the broadening of the Bragg width, both longitudinal and transverse Bragg profile also tend to have more spectral weight in the tails, as observed in the (111) transverse scans.

In Fig. 6, the relative longitudinal and transverse Bragg width ($\delta q/q$) for the (111) and (002) peaks are plotted. The Bragg width of the (111) peak does not vary much with temperature. However, around the (002) peak, a clear onset of both longitudinal and transverse

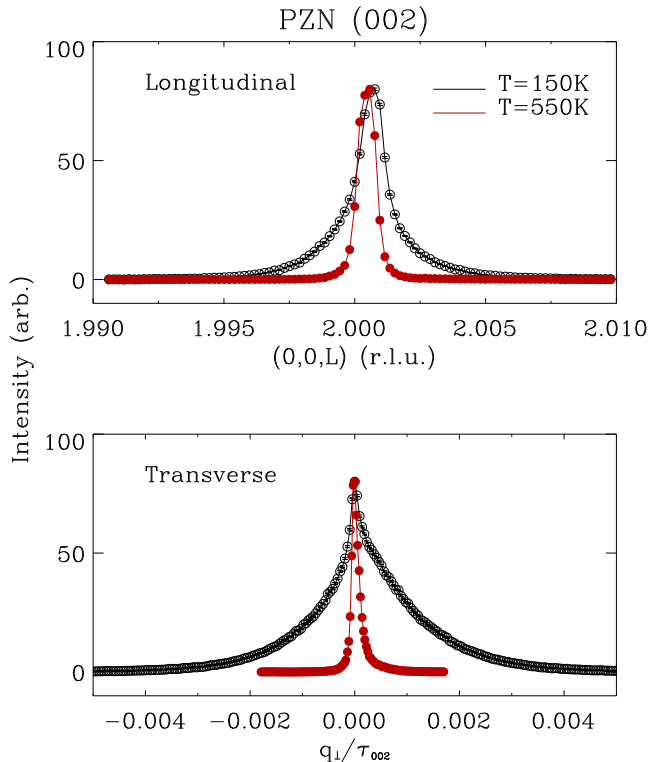


FIG. 5: Longitudinal and transverse scans through the (002) Bragg peak, measured at temperatures above and below T_C with 67 keV x-rays.

Bragg width occurs at T_C , and they increase monotonically upon cooling. The change of the Bragg profile from Gaussian shape to the Lorentzian shape also occurs at around the same temperature. These results indicate that some structural change occurs at T_C , but not so strong as to induce a global lattice distortion.

IV. DISCUSSIONS

The structure of the inside of the pure PZN single crystal with an undistorted lattice has also been discovered lately in another family of relaxor ferroelectrics, a close analog of PZN- x PT, PMN- x PT ($\text{Pb}(\text{Mg}_{1/3}\text{Nb}_{2/3})\text{O}_3$ - x PbTiO_3). High q -resolution neutron scattering measurements by Gehring *et al.* and Xu *et al.* found that phase X is also present in PMN-10%PT¹³ and PMN-20%PT¹⁴ below the Curie temperatures. With increasing PT concentration x , the low temperature phase eventually becomes rhombohedral in PMN-27%PT. These results suggest that phase X is not an exception, but rather a universal phase which is the ground state for PZN- x PT and PMN- x PT systems of small PT concentrations. Pure PMN, which was considered to remain cubic for temperatures as low as 5 K^{15,16}, is likely an extreme case of phase X with very thin outer-layers (so that even Cu K_α x-rays

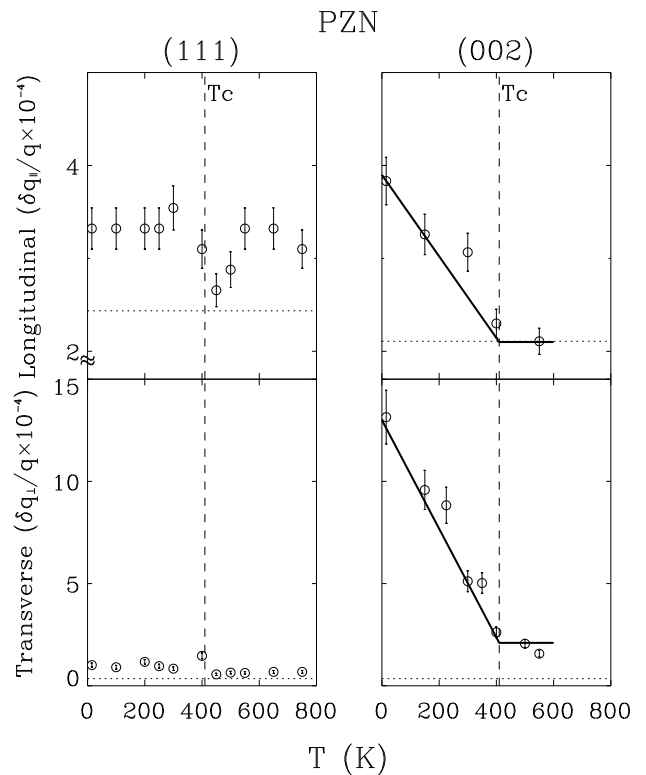


FIG. 6: Longitudinal and transverse Bragg widths (full width at half maximum) at (111) and (002) peaks, measured at different temperatures. The dotted horizontal lines indicate the instrument resolution, and the vertical dashed lines denotes the Curie temperature T_C .

would be able to see the inside undistorted structure).

A. Decoupling of polarization and lattice distortion

Another important fact about phase X is the presence of ferroelectric polarization, as evidenced by the recovery of soft ferroelectric TO phonon below T_C . In the low temperature phase, the energy squared ($(\hbar\omega)^2 \propto 1/\epsilon$) of the zone center TO phonon in both PMN¹⁷ and PZN¹¹ increases linearly upon cooling, a unique behavior of ferroelectrically ordered system. The exact same recovery of the TO mode was also confirmed by Raman measurements by Bovtun *et al.*¹⁸. Note that direct measurements of the polarization - atomic shifts inside the crystal, are difficult because of strong extinction and other reasons. But many indirect measurements show results in support of the ferroelectric polar order below T_C . In addition to the phonon measurements, recent NMR¹⁹ measurements also showed a clear increase of the line intensity corresponding to [111] Pb shifts at T_C , suggesting the development of ferroelectric polarization. In this phase, the internal degree of freedom of the structure - ferroelectric polarization, i.e., atomic shifts, is decoupled from the ex-

ternal degree of freedom - unit cell shape, that can be directly measured by diffraction experiments. While the polarization, as the primary order parameter, show signs of a phase transition into a ferroelectric phase at T_C , the unit cell shape remains cubic. Recent reports on epitaxial films of SrTiO₃²⁰ show similar decoupling effects. There the internal degree of freedom - the rotation of the TiO₆ octahedra, can be directly measured by monitoring the superlattice diffraction peak, and clearly shows a phase transition. Yet the unit cell size and shape do not show any indication of this transition. This decoupling is possibly due to epitaxial strain and substrate clamping effects. The discovery of phase X is the first experimental realization of the decoupling between lattice distortion and ferroelectric polarization inside a *free-standing* crystal.

One unique feature for relaxors is the existence of the polar nano-regions (PNR). These are nano-meter sized local polarized regions that appear at temperatures a few hundred degrees above T_C ²¹. Studies on diffuse scattering intensities indicate that the PNR are in fact displaced from the surrounding lattice. This was first pointed out by Hirota *et al.*²², and the displacement of the PNR is called the “uniform phase shift”. This shift makes the PNR out-of-phase from the whole lattice, and therefore creates an energy barrier, that competes with the ferroelectric polarization and prevents the whole lattice from being (rhombohedrally) distorted. More detailed discussion about the uniform phase shift and its role on the decoupling between the lattice distortion and ferroelectric polarization can be found in Ref. 14. Here we would like to focus on the roles that those PNR play on other properties of phase X.

B. Thermal expansion

The temperature dependence of lattice parameters for those systems with this undistorted phase X present are very similar to each other, but deviate from the typical behavior of ferroelectrics. The lattice parameters have been measured in pure PMN²³, PMN-10%PT¹³, and PMN-20%PT¹⁴. They remain rather constant at low temperatures, and do not change much even above T_C . Only when the temperature is significantly above T_C , we start to see signs of clear thermal expansion. The “onset” temperature is about 500 K for PMN, 450 K for PMN-10%PT, and 400 K for PMN-20%PT, all of them are hundreds of degrees above their Curie temperatures ($T_C \approx 210$ K, 285 K, and 300 K, respectively), and seem to decrease with increasing PT concentration. In our measurements on pure PZN, however, no “onset” has yet been observed (see Fig. 3). Considering the relatively high Curie temperature $T_C \approx 410$ K, this onset temperature could be quite high, even beyond our current experimental capabilities (750 K). Taking into account the difference in T_C between PZN and PMN, we find that the temperature dependence of the lattice parameter in those two compounds are in close resemblance - constant

lattice parameter from low temperature up to ~ 300 K above T_C .

The reason for this intriguing behavior is, nevertheless, not yet clear to us. It is in contrary to the known thermal expansion property of any ferroelectric oxide. On the other hand, we note that the change of lattice parameters of the inside structure, may not be equivalent to that of a macroscopic thermal expansion measurement. The outer-layer has an entirely different temperature dependence. Another interesting point is that the lattice parameter of the outer-layer is actually smaller than that of the inside. Recent narrow beam neutron scattering measurements²⁴ also indicated similar behavior (small outer-layer lattice parameter than the inside) in a single crystal of PMN-*x*PT. It is possible that this can create a clamping effect, like the substrate clamping effects on the SrTiO₃ thin films²⁰. In that case, the inside lattice would be under external constraints, while the whole crystal is still “free-standing”. With the structural phase transition at T_C , the growing mismatch between the outer-layer and inside structures may also induce additional strain and stress inside the crystal.

C. Structural inhomogeneity

Phase X is also unusual in the way that structural changes occur at the phase transition without any macroscopic lattice distortion. Previous report by Mulvihill *et al.*²⁵ suggests that below T_C , PZN could be in a “microdomain” state, with $< 0.1 \mu\text{m}$ sized rhombohedral microdomains. Our data indicate that those rhombohedral “microdomains” are very likely to exist, but only in the “outer-layer”. Inside the crystal, the unit cell shape remains cubic. The Bragg peaks, especially the (002) peak, does broaden below T_C . If we attribute this broadening to the finite size effect of “microdomains”, the size of those domains can be estimated from the Bragg width. For example, at $T = 15$ K, the FWHM of the (002) Bragg peak in the longitudinal direction is $2\Gamma \sim 0.0012 \text{ \AA}^{-1}$, corresponding to an average domain size of $L = 0.94\pi/\Gamma \approx 5000 \text{ \AA}$. This is much larger than the size of “microdomains”. Also consider the fact that neutron scattering measurements¹¹ yield much larger (~ 5 times) Bragg widths, after the resolution has been taken into account. It is highly unlikely that the “domain size” seen by neutrons would be much smaller than that seen by x-rays.

A more feasible explanation is that the broadening are due to strains caused by structural inhomogeneity in the lattice. The source of the inhomogeneity is the PNR. At temperatures above T_C , although PNR already exist, the interaction between the PNR and the unpolarized surrounding lattice is not significant. When cooling below T_C , as shown by neutron diffuse scattering²⁶ and specific heat²⁷ measurements on PMN, both the size and total volume of the PNR increase rapidly. It is reasonable to believe that this is also the case in PZN. The ferroelectric

polarization established in the whole lattice will then interact much more strongly with the “out-of-phase” PNR, trying to pull them back in-phase. The competition between this interaction and the energy barrier created by the uniform phase shift induces strain and stress in the lattice. The lower the temperature, the stronger the interaction and the strain. Moreover, the PNR and this interaction is apparently not isotropic, as the PNR and the surrounding lattice are polarized along certain crystallographic orientations. This leads to the difference between strain measured at different Bragg peaks. In our x-ray measurements, the longitudinal Bragg broadening, which is related to the strain, is much less along the (111) direction than the (002) direction. In fact, high q -resolution neutron scattering measurements have been performed on this same PZN single crystal at 300 K, on the (111) Bragg peak. The peak remains single, with much smaller broadening than that obtained by neutron measurements on (110) and (002) peaks.

The Bragg width and lineshape also change at T_C in the transverse direction. A transverse scan is used to measure the sample “mosaic”. Usually, the mosaic of a crystal is the result of defects and dislocations in the lattice, which make the adjacent domains align at slightly different angles. The macroscopic result is a broadening of the crystal mosaic. In the case of PZN, the transverse inhomogeneity, or, the effective “mosaic”, is more related to the PNR as local “defects”. This is different from the original concept of mosaic. The presence of the PNR, and more importantly, their increasing interactions with the surrounding regions, create not only strains, but also an increasing transverse inhomogeneity with cooling. Similar to the strain, the transverse inhomogeneity is also anisotropic, and has strong dependence on the crystallographic orientations. This effective “mosaic” created by the PNR propagates through the whole crystal. In fact, if we only look at a small part of the crystal, only a portion of the total inhomogeneity is actually being measured. The fact that neutron measurements¹¹ yield larger values of both longitudinal and transverse Bragg

widths than our x-ray measurements can be reconciled by considering the total volume of crystal in the beam. Neutron beam sizes are much larger and usually covers the whole crystal, and will be sensitive to the large inhomogeneity of the whole crystal. X-ray beams, on the other hand, are much smaller (our typical beam size ~ 0.5 mm in diameter), and only probes a very small part of the crystal.

Overall, our high energy x-ray studies on the inside structure of single crystal PZN reveals a phase with unique lattice properties. The unit cell remains cubic shape below T_C , while instability and effective mosaic in the lattice increase significantly with cooling at and below the phase transition. The lattice parameter of the inside lattice remains almost constant for the whole temperature range from 15 K to 750 K, in contrary to the thermal expansion behavior of any known ferroelectric oxide. These anomalous behaviors are not fully understood yet, and further investigations are underway. There is also an outer-layer structure that is entirely different and behaves consistently with a typical ferroelectric system. We speculate that the inside phase is the true ground state of PZN and similar relaxor systems with low PT dopings. Its behaviors are much dominated by the interactions of the phase shifted PNR and the surrounding lattice, and thus highly unusual.

Acknowledgments

We would like to thank A. A. Bokov, P. M. Gehring, S. M. Shapiro, S. B. Vakrushev, and D. Viehland for stimulating discussions. Financial support from the U.S. Department of Energy under contract No. DE-AC02-98CH10886, U.S. Office of Naval Research Grant No. N00014-99-1-0738, and the Natural Science and Research Council of Canada (NSERC) is also gratefully acknowledged.

¹ S.-E. Park and T. R. Shrout, *J. Appl. Phys.* **82**, 1804 (1997).

² J. Kuwata, K. Uchino, and S. Nomura, *Jpn. J. Appl. Phys.* **21**, 1298 (1982).

³ J. Kuwata, K. Uchino, and S. Nomura, *Ferroelectrics* **37**, 579 (1981).

⁴ B. Noheda, D. E. Cox, G. Shirane, S.-E. Park, L. E. Cross, and Z. Zhong, *Phy. Rev. Lett.* **86**, 3891 (2001).

⁵ D. E. Cox, B. Noheda, G. Shirane, Y. Uesu, K. Fujishiro, and Y. Yamada, *Appl. Phys. Lett.* **79**, 400 (2001).

⁶ D. La-Orautapong, B. Noheda, Z.-G. Ye, P. M. Gehring, J. Toulouse, D. E. Cox, and G. Shirane, *Phys. Rev. B* **65**, 144101 (2002).

⁷ Y. Uesu, M. Matsuda, Y. Yamada, K. Fujishiro, D. E. Cox, B. Noheda, and G. Shirane, *J. Phys. Soc. Jpn.* **71**, 960 (2002).

⁸ A. Lebon, H. Dammak, G. Calvarin, and I. O. Ahmedou, *J. Phys.: Condens. Matter* **14**, 7035 (2002).

⁹ G. Xu, Z. Zhong, Y. Bing, Z.-G. Ye, C. Stock, and G. Shirane, *Phys. Rev. B* **67**, 104102 (2003).

¹⁰ G. Xu, H. Hiraka, K. Ohwada, and G. Shirane (2004), *cond-mat/0401437*.

¹¹ C. Stock, R. J. Birgeneau, S. Wakimoto, J. S. Gardner, W. Chen, Z.-G. Ye, and G. Shirane, *Phys. Rev. B* **69**, 094104 (2004).

¹² Y.-H. Bing, A. A. Bokov, Z.-G. Ye, B. Noheda, and G. Shirane (2004), unpublished.

¹³ P. M. Gehring, W. Chen, Z.-G. Ye, and G. Shirane (2003), *cond-mat/0304289*.

¹⁴ G. Xu, D. Viehland, J. F. Li, P. M. Gehring, and G. Shirane, *Phys. Rev. B* **68**, 212410 (2003).

¹⁵ P. Bonneau, P. Garnier, E. Husson, and A. Morell, *Mater.*

- Re. Bull **24**, 201 (1989).
- ¹⁶ N. de Mathan, E. Husson, G. Calvarin, J. R. Gavarri, A. W. Hewat, and A. Morell, *J. Phys. Condens. Matter* **3**, 8159 (1991).
- ¹⁷ S. Wakimoto, C. Stock, R. J. Birgeneau, Z.-G. Ye, W. Chen, W. J. L. Buyers, P. M. Gehring, and G. Shirane, *Phys. Rev. B* **65**, 172105 (2002).
- ¹⁸ V. Bovtun, S. Kamba, A. Pashkin, and M. Savinov (2003), proceedings of NATO Advanced Research Workshop on the Disordered Ferroelectrics, Kiev.
- ¹⁹ R. Blinc, V. Laguta, and B. Zalar, *Phys. Rev. Lett.* **91**, 247601 (2003).
- ²⁰ F. He, B. O. Wells, S. M. Shapiro, M. v. Zimmermann, A. Clark, and X. X. Xi, *Appl. Phys. Lett.* **83**, 123 (2003).
- ²¹ G. Burns and F. H. Dacol, *Phys. Rev. B* **28**, 2527 (1983).
- ²² K. Hirota, Z.-G. Ye, S. Wakimoto, P. M. Gehring, and G. Shirane, *Phys. Rev. B* **65**, 104105 (2002).
- ²³ J. Zhao, A. E. Glazounov, Q. M. Zhang, and B. Toby, *Appl. Phys. Lett.* **72**, 1048 (1998).
- ²⁴ K. Conlon and C. Stock, private communications.
- ²⁵ M. L. Mulvihill, L. E. Cross, W. Cao, and K. Uchino, *J. Am. Ceram. Soc* **80**, 1462 (1997).
- ²⁶ G. Xu, G. Shirane, J. R. D. Copley, and P. M. Gehring, *Phys. Rev. B* **69**, 064112 (2004).
- ²⁷ Y. Moriya, H. Kawaji, T. Tojo, and T. Atake, *Phys. Rev. Lett.* **90**, 205901 (2003).